

## Electronic Supplementary Information

### **Multi-mode enhanced Raman scattering spectroscopy using aggregation-free hybrid metal/metal-oxide nanoparticles with intrinsic oxygen vacancies**

*Gemma Davison, Yidan Yin, Tabitha Jones, Ivan P. Parkin, William J. Peveler\*, Tung-Chun Lee\**

G. Davison, Y. Yin, T. Jones, T.-C. Lee

Institute for Materials Discovery, University College London, London, WC1H 0AJ, UK

E-mail: [tungchun.lee@ucl.ac.uk](mailto:tungchun.lee@ucl.ac.uk)

G. Davison, Y. Yin, T. Jones, I. P. Parkin, T.-C. Lee

Department of Chemistry, University College London, London, WC1H 0AJ, UK

W. J. Peveler

School of Chemistry, University of Glasgow, Glasgow, G12 8QQ, UK

E-mail: [william.peveler@glasgow.ac.uk](mailto:william.peveler@glasgow.ac.uk)

## Table of Contents

<i>Materials and Synthesis</i> .....	3
<b>Gold nanotriangles</b> .....	3
<b>Au-SnO<sub>2</sub></b> .....	3
<i>Instrumentation</i> .....	3
<b>Ultraviolet-Visible Spectroscopy</b> .....	3
<b>Transmission Electron Microscopy</b> .....	4
<b>X-ray Photoelectron Spectroscopy</b> .....	4
<b>Powder X-ray Diffraction</b> .....	4
<b>Raman Spectroscopy</b> .....	4
<i>Additional Figures – Au NT optical, EM and XRD characterisation</i> .....	6
<i>Additional Figures – XPS Characterisation</i> .....	13
<i>Additional Figures – Raman, SERS and PIERS characterisation</i> .....	16

## **Materials and Synthesis**

Hexadecyltrimethylammonium chloride (CTAC), potassium iodide (KI), gold(III) chloride solution ( $\text{HAuCl}_4$ ), 4-mercaptobenzoic acid (4-MBA), 2,4-dinitrotoluene (DNT), and L-ascorbic acid (AA) were all purchased from Sigma-Aldrich/Merck. Sodium stannate trihydrate and potassium iodide (KI) was purchased from Alfa Aesar. Sodium hydroxide (NaOH) was from Fisher Scientific. All chemicals were used as received, and Milli-Q water was used in all experiments.

### **Gold nanotriangles**

For the synthesis of Au NTs 1.6 mL of 0.1 M CTAC was diluted with 8 mL water and placed in a thermomixer at room temperature under gentle mixing at 300 rpm. 75  $\mu\text{L}$  of 0.01 M potassium iodide was added, then 80  $\mu\text{L}$  of 25.4 mM  $\text{HAuCl}_4$  and 20  $\mu\text{L}$  of 0.1 M NaOH were then mixed together and also added to the solution. 80  $\mu\text{L}$  of ascorbic acid was then added, and 10  $\mu\text{L}$  of 0.1 M NaOH was injected with the rpm increased to 1000 for a few seconds. After approximately 10 minutes the solution turned purple in color and the synthesis was complete.<sup>[1]</sup>

### **Au-SnO<sub>2</sub>**

The pH of 10 mL of the previously prepared Au NTs was adjusted to 10.5 by adding approximately 20  $\mu\text{L}$  of 1 M sodium hydroxide, monitored using a Mettler Toledo FiveEasy pH meter. This solution was then mixed with 2 mL of 0.4 mM sodium stannate for 5 minutes in a thermomixer at 600 rpm, followed by heating to 60 °C and maintaining the solution at this temperature for 1 hour under rapid mixing at 800 rpm. The Au NT-SnO<sub>2</sub> was then centrifuged and re-dispersed in water, before the procedure was repeated to form additional layers of coating.<sup>[2]</sup>

## **Instrumentation**

### **Ultraviolet-Visible Spectroscopy**

An Ocean Optics spectrometer was used to acquire UV-vis spectra of the samples. Milli-Q water was used to store a reference spectrum and a background spectrum. The Au NT-SnO<sub>2</sub> solution was transferred into a 1 cm optical path length cuvette and placed in the spectrometer for measurements. A 10 ms integration time was used, with 300 scans to average, and a boxcar width of 3. The extinction spectra were collected in a wavelength range of 180 - 880 nm.

### **Transmission Electron Microscopy**

A JEOL 2100 200 kV TEM with an Orius SC200 camera was used to obtain images of the samples. A pipette was used to transfer a few drops of the Au NT-SnO<sub>2</sub> solution onto a Holely carbon TEM grid (300-mesh, Cu), which was then left to air dry. Gatan digital micrograph software was used to analyze the images obtained.

### **X-ray Photoelectron Spectroscopy**

A Thermo K-Alpha X-ray Photoelectron Spectrometer (XPS) system was used to characterize the samples. The Au NT-SnO<sub>2</sub> solution was centrifuged and drop-cast onto a 0.5 cm<sup>2</sup> glass substrate and left to air dry. This was then secured onto a sample plate using carbon tape and placed in the X-ray Photoelectron Spectrometer. CasaXPS software was used to analyze the data.

### **Powder X-ray Diffraction**

To prepare the samples for powder X-ray diffraction (PXRD), Au NT-SnO<sub>2</sub> solutions were centrifuged, the solvent was removed using a pipette, and the remaining solution was left to air dry to form a powder. The powder was then placed in an aperture holder and into the PXRD. A Stoe STADI-P geometry system with molybdenum (Mo K $\alpha$ 1,  $\lambda = 0.7093 \text{ \AA}$ ) radiation was used, with 50 kV and 30 mA.

### **Raman Spectroscopy**

An Ocean Optics Raman spectrometer with a 632.8 nm helium-neon laser and a laser power of 22 mW was used for taking the spectra. For PIERS, a 365-nm UV LED with 12.5 mW power

was used to in situ irradiate the substrate with a light path perpendicular to that of the Raman laser. Stock solutions of 2,4-dinitrotoluene (DNT) in water at concentrations of 1  $\mu$ M and 1 mM were prepared. These were then mixed with the Au NT-SnO<sub>2</sub> solutions at various concentrations and 1 mL of solution was placed in a cuvette for measurements. Ten accumulations of 7 s scans were acquired on each measurement. Five measurements were taken per sample. The spectra were averaged and baseline was corrected using an asymmetric least-squares (ALS) plugin in Origin.

### Additional Figures – Au NT optical, EM and XRD characterisation

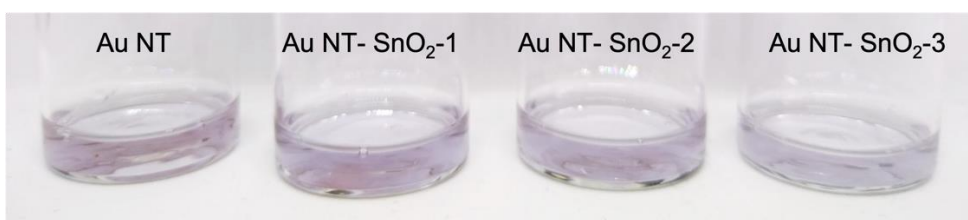


Figure S1: Solutions of (L to R) Au NTs, Au NT-SnO<sub>2</sub>-1, Au NT-SnO<sub>2</sub>-2 and Au NT-SnO<sub>2</sub>-3.

Au NTs are in 17 mM aqueous CTAC, Au NT-SnO<sub>2</sub>-1/2/3 are in water.

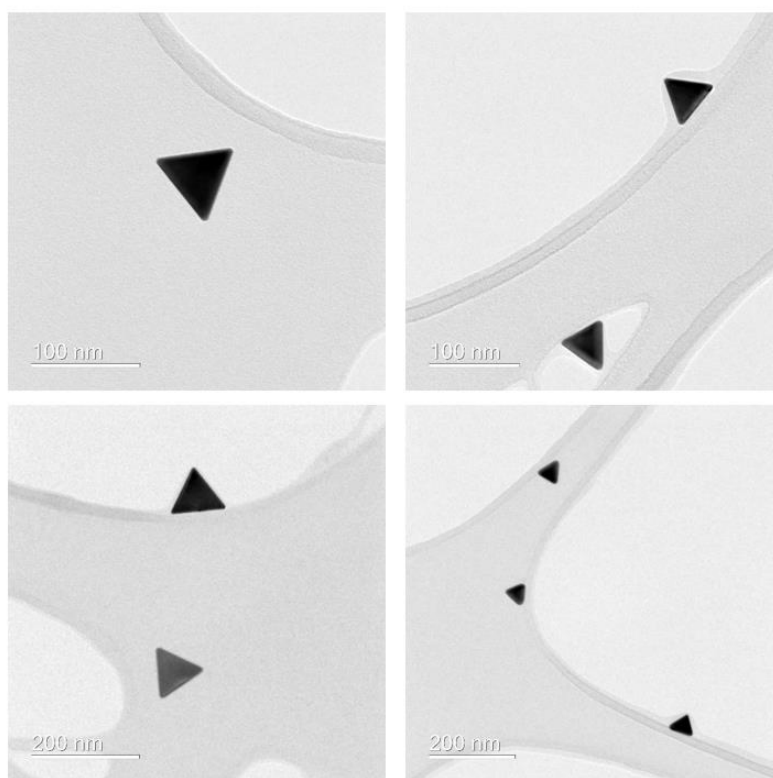


Figure S2: Bright-field TEM images of Au NTs.

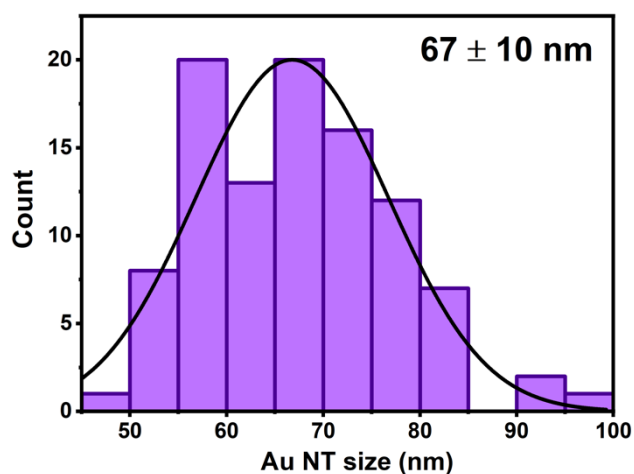


Figure S3: Side lengths distribution of Au NTs measured from 100 particles in the TEM images, using Gatan Digital Microscopy software.

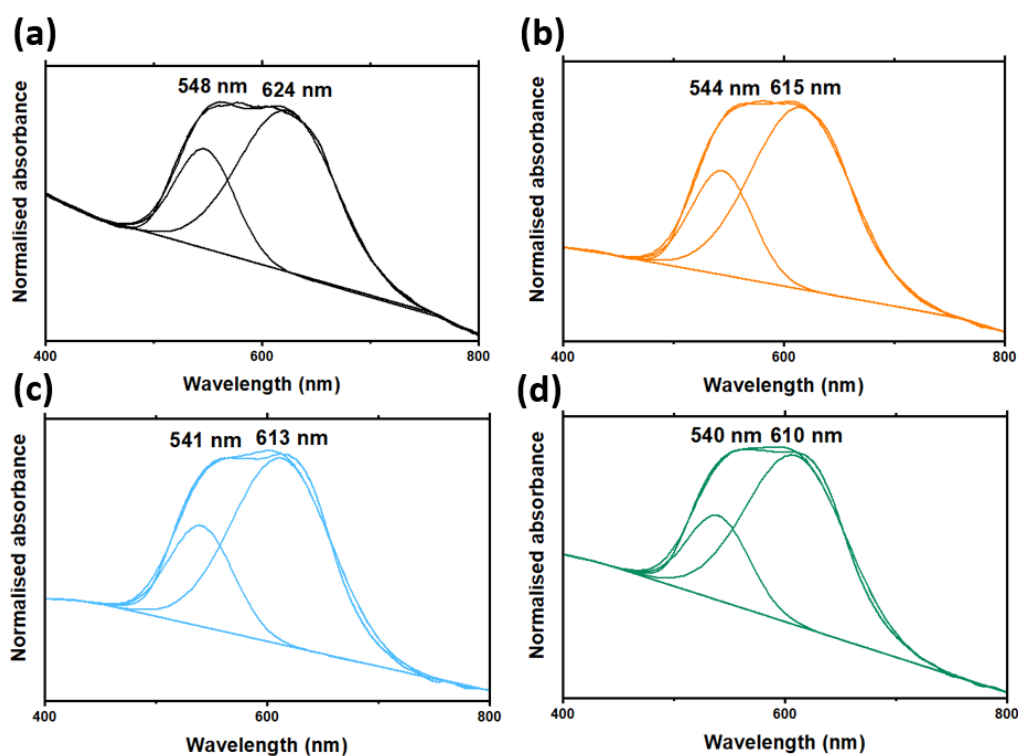


Figure S4: Deconvoluted UV-vis extinction spectra of (a) Au NTs, (b) Au NT-SnO<sub>2</sub>-1, (c) Au NT-SnO<sub>2</sub>-2, and (d) Au NT-SnO<sub>2</sub>-3. Au NTs are in 17 mM aqueous CTAC, Au NT-SnO<sub>2</sub>-1/2/3 are in water.

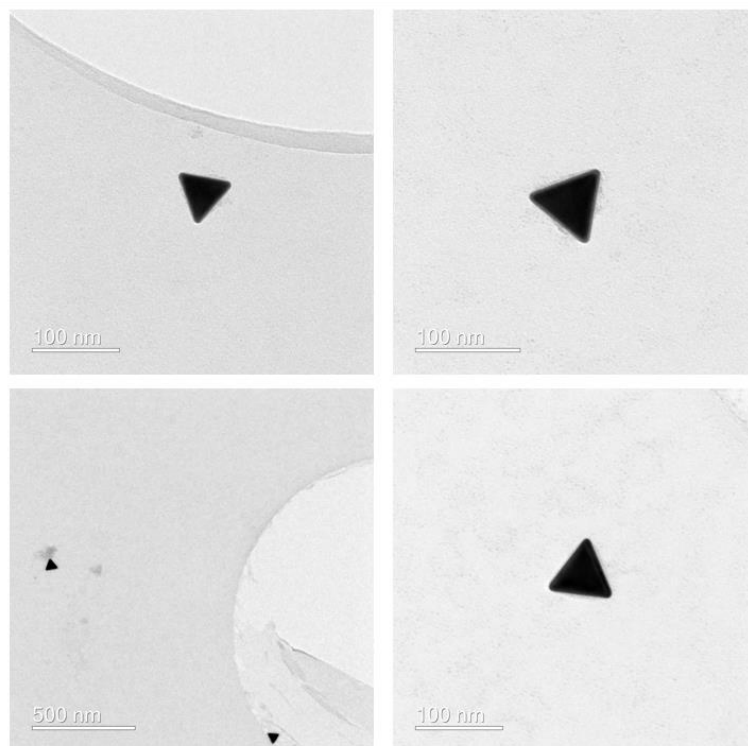


Figure S5: TEM images of Au NT-SnO<sub>2</sub>-1 with one SnO<sub>2</sub> coating cycle.

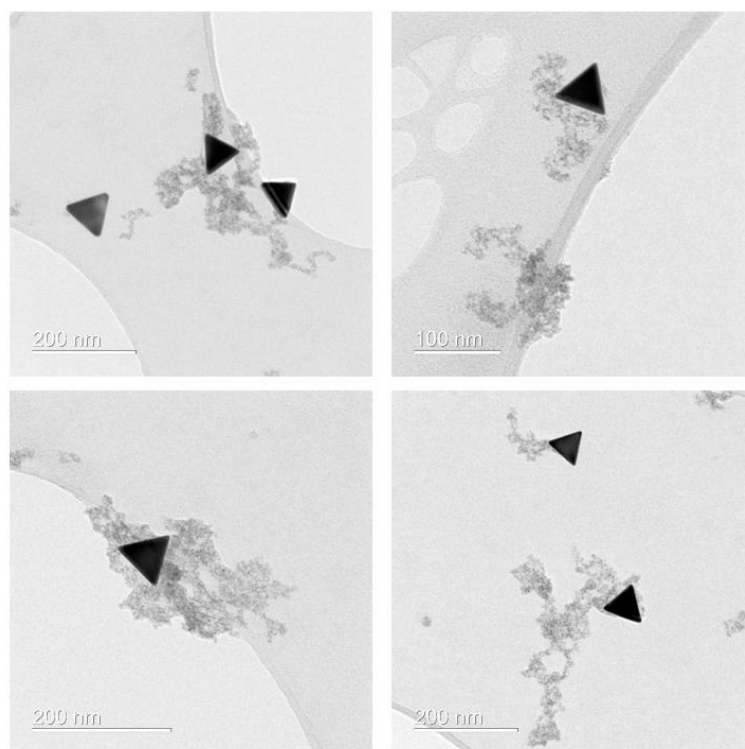


Figure S6: TEM images of Au NT-SnO<sub>2</sub>-2 with two SnO<sub>2</sub> coating cycles.



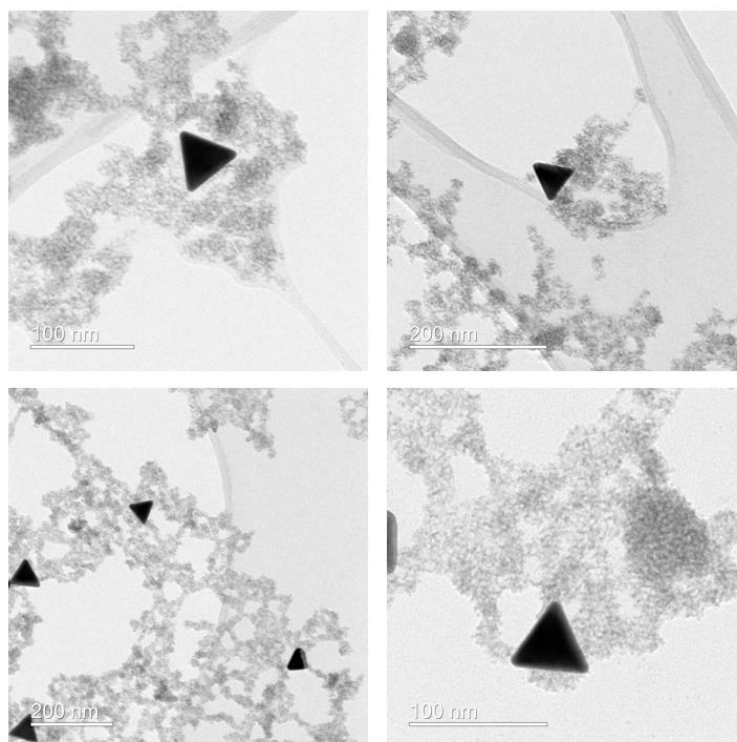


Figure S7: TEM images of Au NT-SnO<sub>2</sub>-3 with three SnO<sub>2</sub> coating cycles.

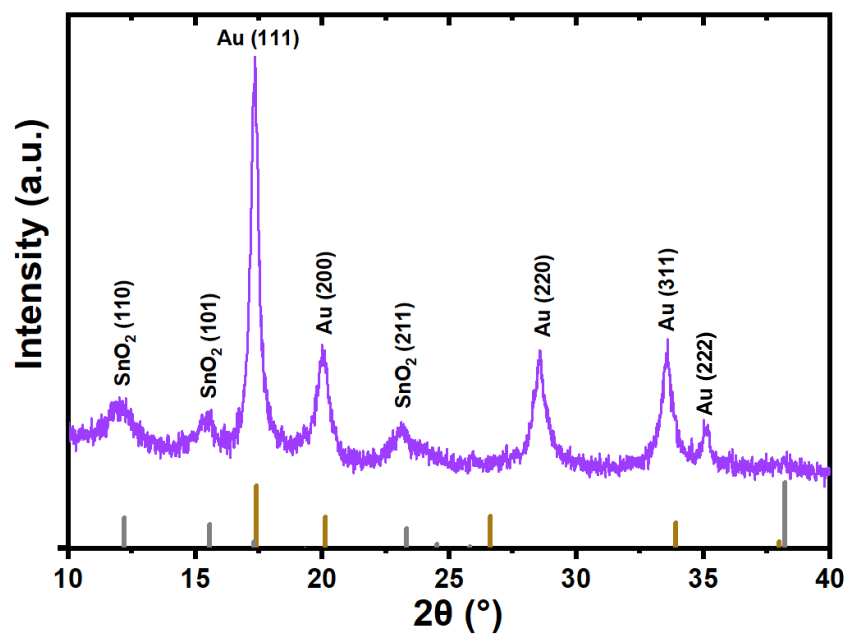


Figure S8: XRD of Au NP@ SnO<sub>2</sub>, using Mo K $\alpha$ 1 source. Grey bars are SnO<sub>2</sub> reference and brown bars the Au reference, as per the main text. The unindexed peak at 35° is likely Au (222).

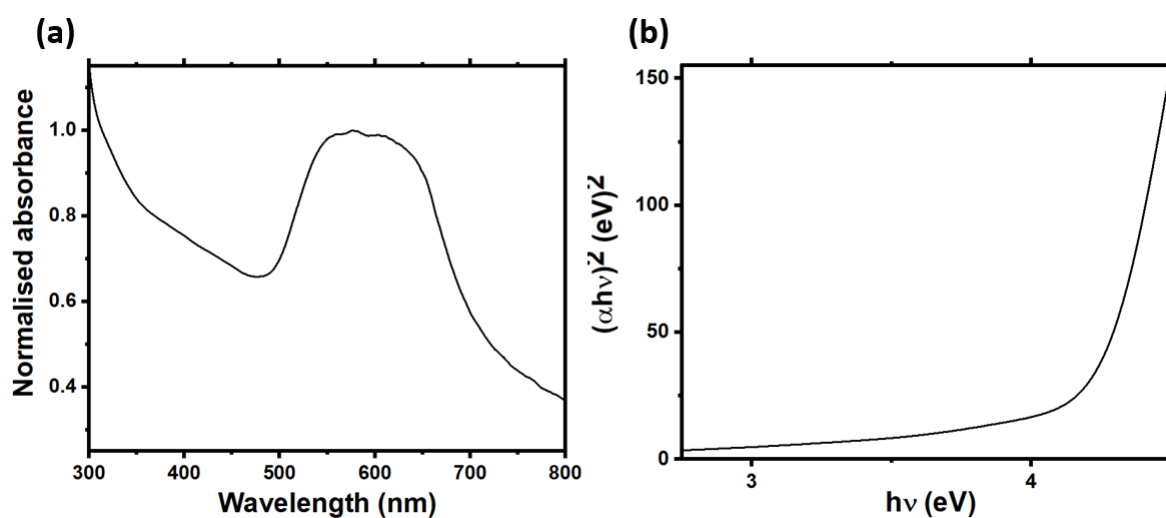


Figure S9: (a) UV-vis extinction spectrum of Au NTs. (b) Tauc plot of Au NTs, with  $h\nu$  and  $(\alpha h\nu)^2$  calculated from the absorbance spectrum. Solvent is 17 mM aqueous CTAC.

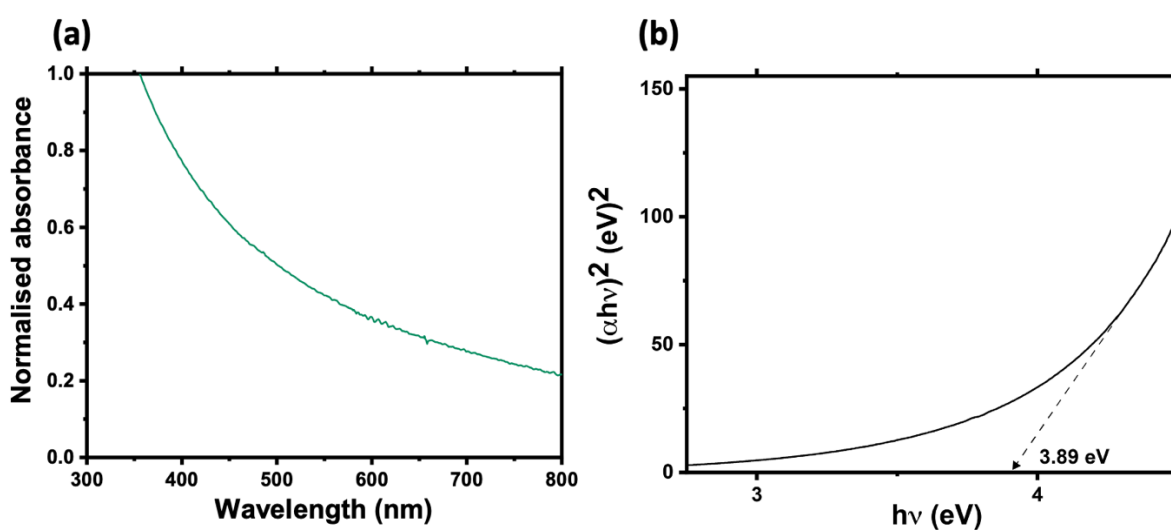


Figure S10: (a) UV-vis extinction spectrum of SnO<sub>2</sub> NPs: (a) UV-vis extinction spectrum of SnO<sub>2</sub> produced from sodium stannate condensation. (b) Tauc plot of SnO<sub>2</sub>, with  $h\nu$  and  $(\alpha h\nu)^2$  calculated from the absorbance spectrum. Solvent is deionized water.

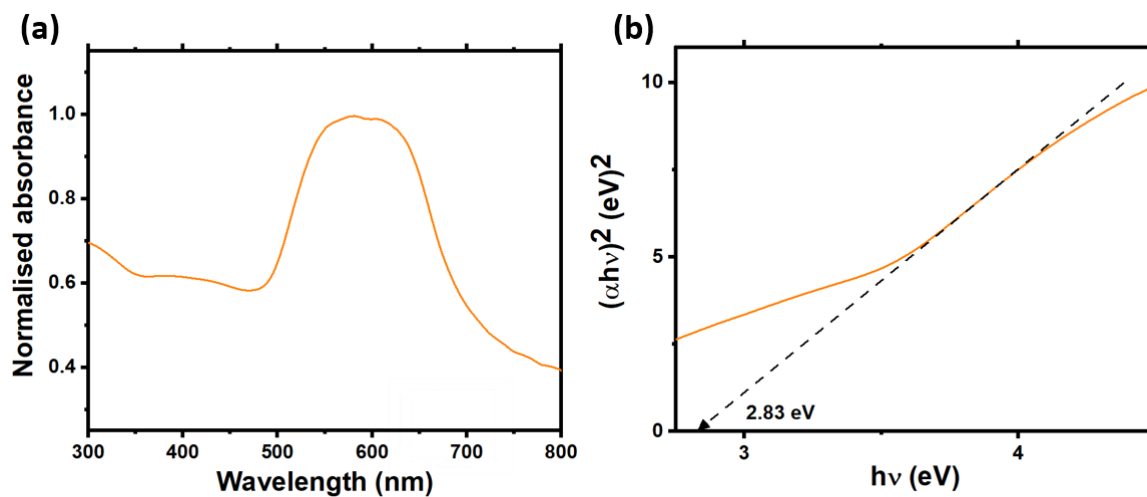


Figure S11: (a) UV-vis extinction spectrum of Au NT-SnO<sub>2</sub>-1. (b) Tauc plot of Au NT-SnO<sub>2</sub>-1. Solvent is deionized water.

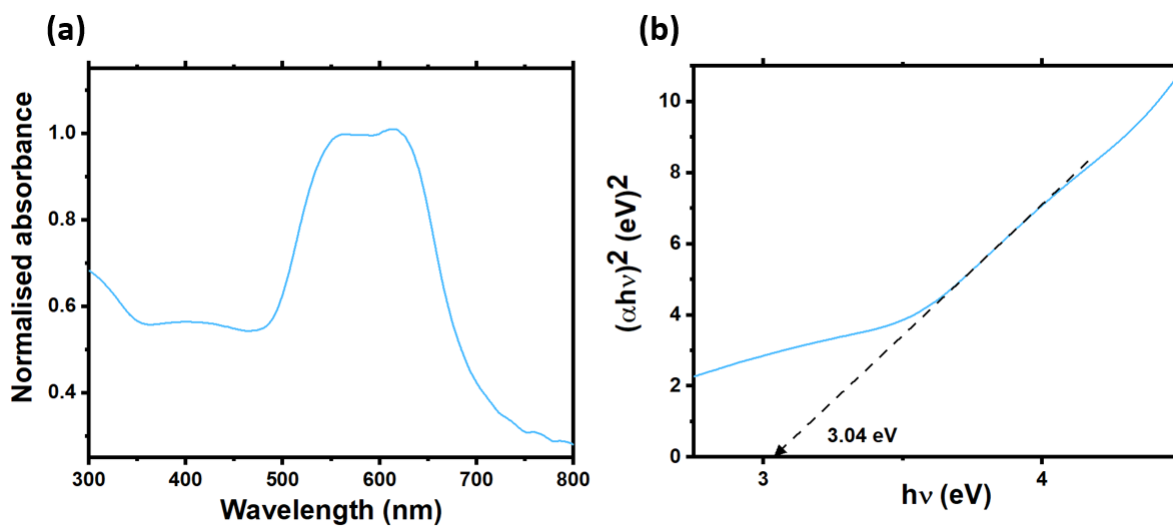


Figure S12: (a) UV-vis extinction spectrum of Au NT-SnO<sub>2</sub>-2. (b) Tauc plot of Au NT-SnO<sub>2</sub>-2. Solvent is deionized water.

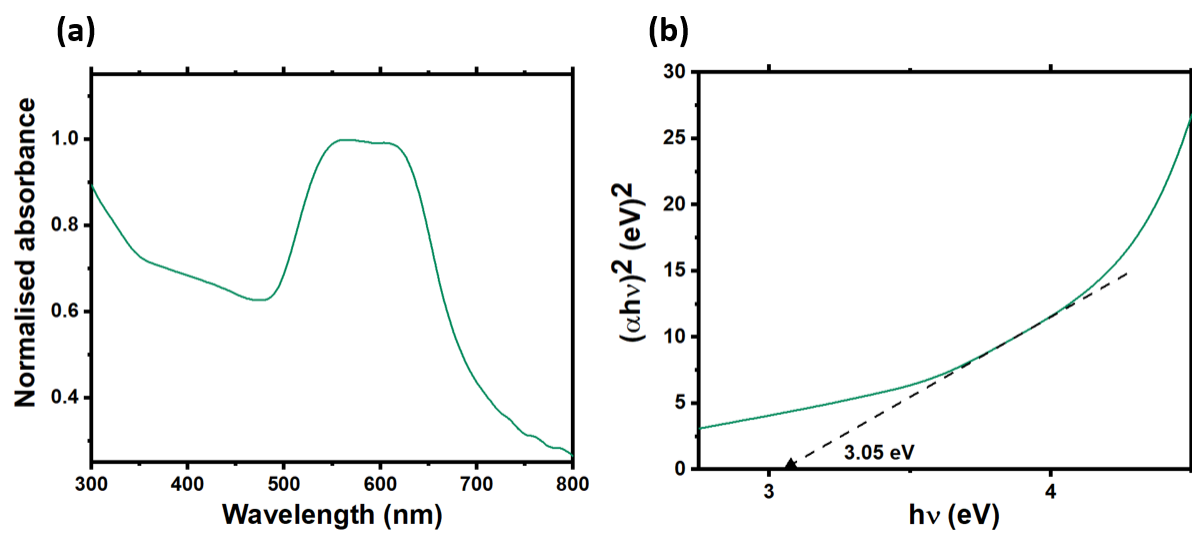


Figure S13: (a) UV-vis extinction spectrum of Au NT-SnO<sub>2</sub>-3. (b) Tauc plot of Au NT-SnO<sub>2</sub>-3. Solvent is deionized water.

## Additional Figures – XPS Characterisation

XPS spectra of Au NT-SnO<sub>2</sub> have very low intensity due to difficulties in scaling up the synthesis (Figure S14). The Sn region (not shown) of the spectrum shows one peak which does not appear to correspond to Sn, but instead results from the Na KLL Auger line. Au 4f displays two peaks of Au 4f<sub>7/2</sub> and Au 4f<sub>5/2</sub>. The synthesis of core@shell Au NP@ SnO<sub>2</sub>, with the SnO<sub>2</sub> coating synthesized using the same method as for the Au NT-SnO<sub>2</sub>, was able to be scaled up and provide a larger quantity of dried sample for XPS measurements (Figure S15). This sample displays Sn 3d<sub>5/2</sub> and Sn 3d<sub>3/2</sub> peaks with the binding energies of oxidized species of Sn, Au 4f<sub>7/2</sub> and Au 4f<sub>5/2</sub> peaks, and similar O 1s peaks to the results from the Au NT-SnO<sub>2</sub>, with O 1s<sub>v</sub> peak of higher intensity than O 1s, indicating the presence of more oxygen vacancies than crystalline SnO<sub>2</sub>. Commercial SnO<sub>2</sub> powder was used to investigate the XPS spectra of crystalline SnO<sub>2</sub>, which had higher intensity O 1s than O 1s<sub>v</sub> as well as Sn 3d<sub>5/2</sub> and Sn 3d<sub>3/2</sub> peaks visible (Figure S16).

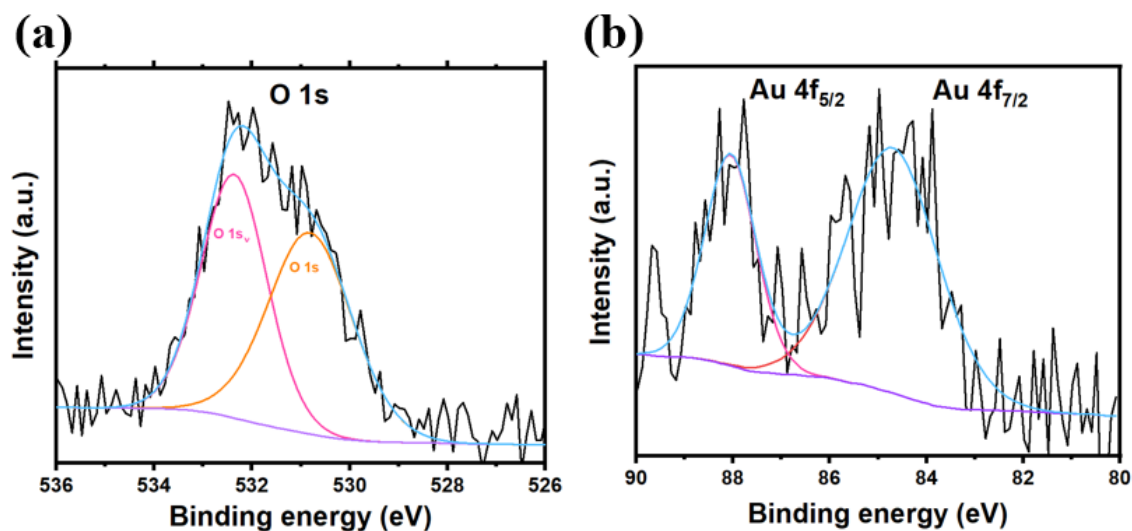


Figure S14: XPS of (a) oxygen 1s peak, and (b) Au 4f peaks, of Au NT-SnO<sub>2</sub>-2.

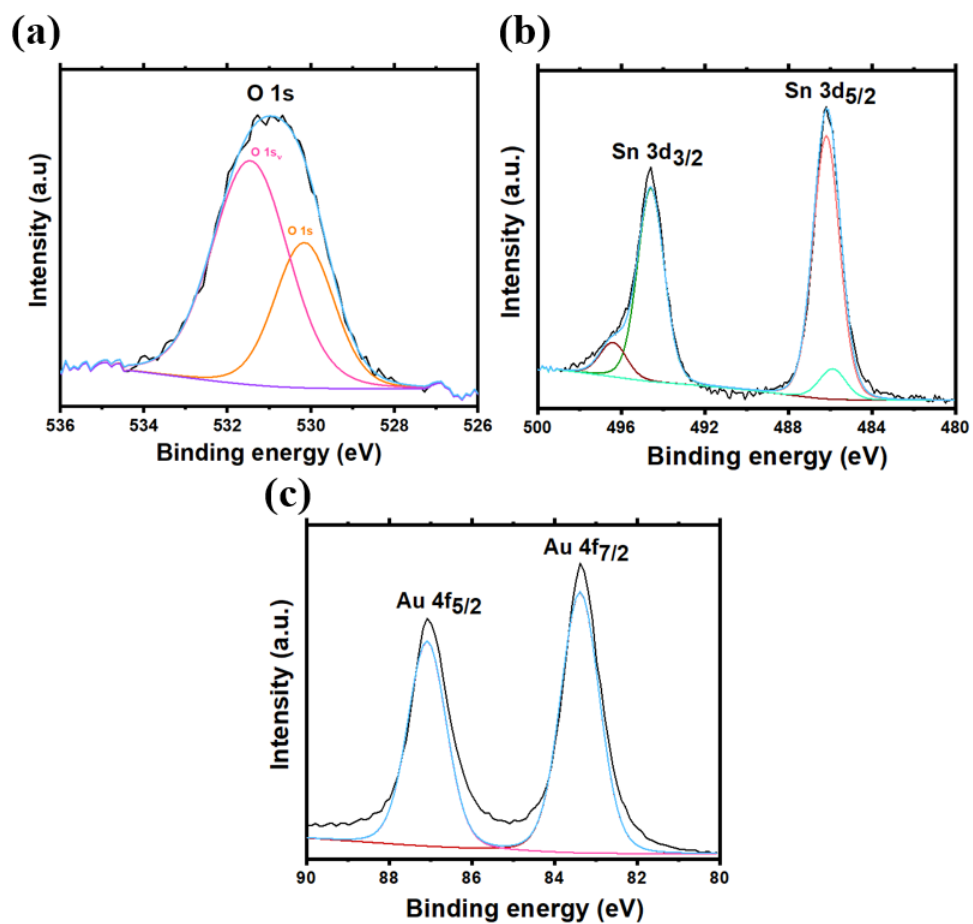


Figure S15: XPS of (a) oxygen 1s peak, (b) Sn 3d peaks, and (c) Au 4f peaks, of Au NP@ SnO<sub>2</sub>.

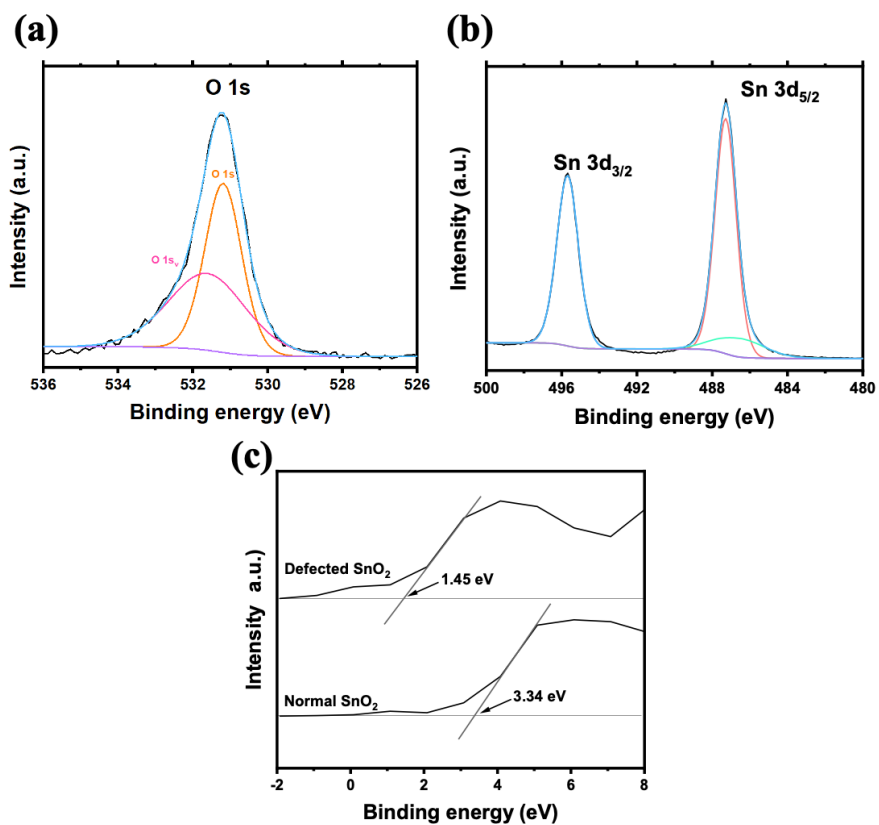


Figure S16: XPS of (a) oxygen 1s peak, and (b) Sn 3d peaks of commercial SnO<sub>2</sub>. (c) Comparison of the valence band of commercial crystalline SnO<sub>2</sub> powder and the "defected" SnO<sub>2</sub> in a sample of Au NT-SnO<sub>2</sub>.

## Additional Figures – Raman, SERS and PIERS characterisation

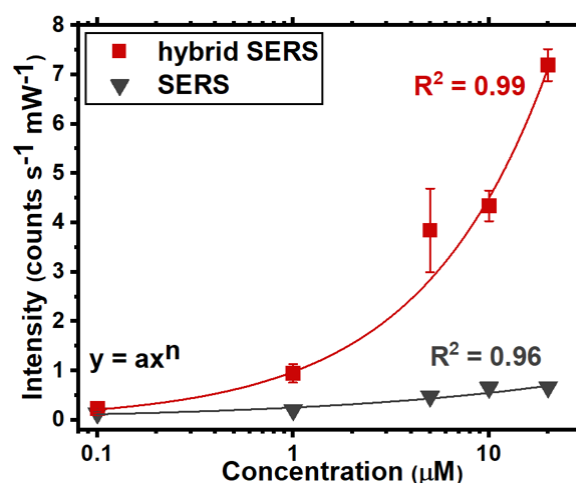


Figure S17: (a) SERS and hybrid SERS spectra of 4-MBA,  $1588\text{ cm}^{-1}$  peak. Solvent is deionized water, and Au NTs are in 17 mM CTAC. Hybrid SERS  $y = 0.98x^{0.66}$ , SERS  $y = 0.25x^{0.34}$

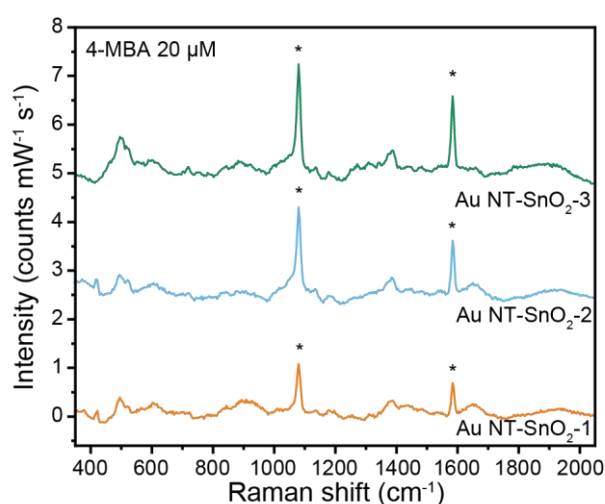


Figure S18: Hybrid SERS spectra of  $20\text{ }\mu\text{M}$  4-MBA in the presence of colloidal Au NT-SnO<sub>2</sub> (at a constant Au NT concentration) with 1–3 coating cycles of SnO<sub>2</sub>. Raman peaks of 4-MBA marked with \*. Solvent was deionized water for Au NT-SnO<sub>2</sub>, and 17 mM aqueous CTAC for Au NTs. Baseline offset for clarity.



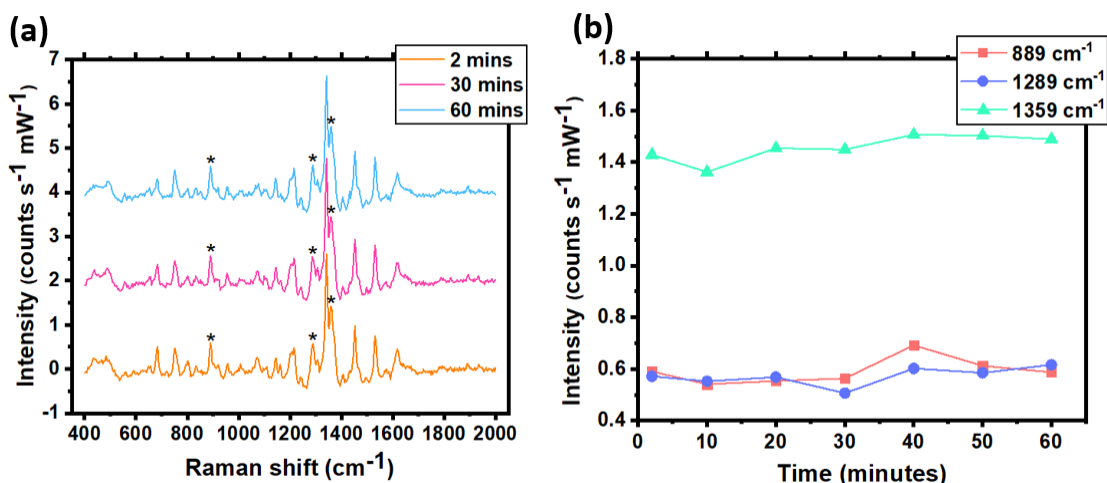


Figure S19: Stability of hybrid SERS signals over 1 hour for DNT. (a) Hybrid-SERS spectra and (b) plot of Raman intensity against time. Solvent is deionized water.

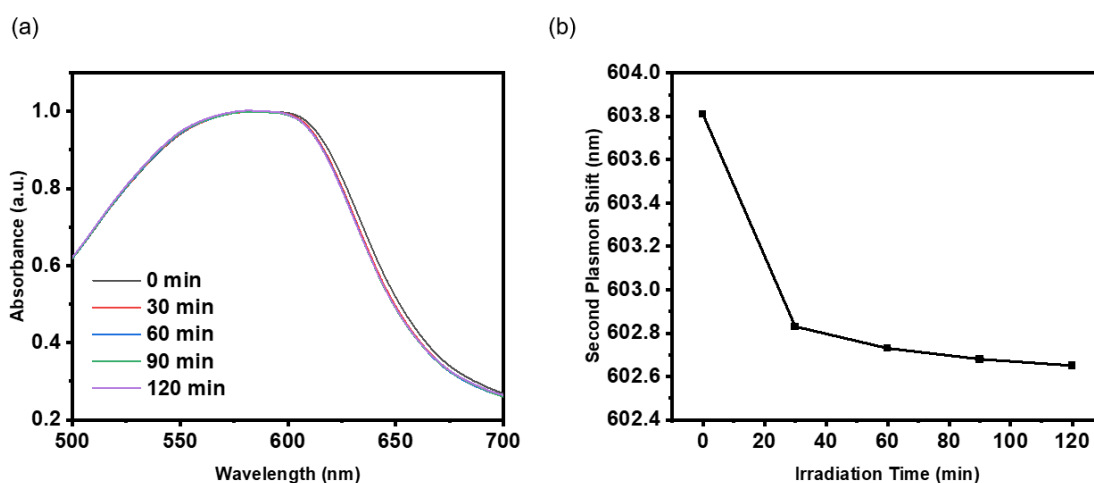


Figure S20: Change in UV-vis extinction of Au NT-SnO<sub>2</sub>-2 over time under 365-nm UV irradiation. The LSPR band consists of two gaussians centered at ca. 540 nm (out-of-plane) and ca. 600 nm (in-plane). The out-of-plane mode does not markedly change but a distinct blue-shift is observed for the in-plane mode upon irradiation.

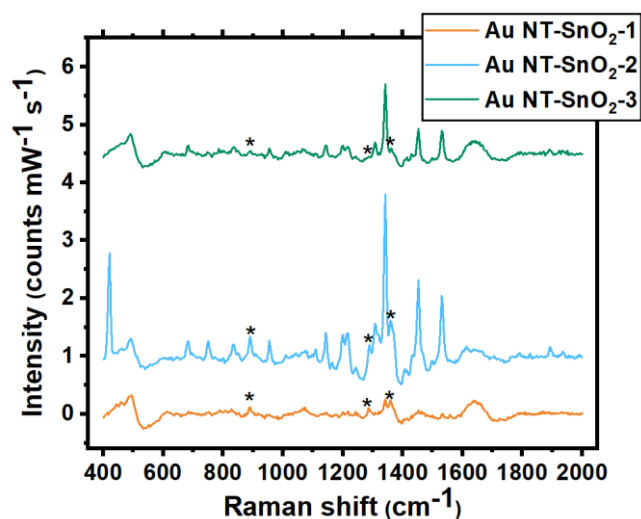


Figure S21: Hybrid SERS spectra of 20  $\mu\text{M}$  DNT in Au NT-SnO<sub>2</sub> (at constant Au NT concentration) with 1–3 coating cycles of SnO<sub>2</sub>. Raman peaks of DNT marked with \* and CTAC with x. Solvent was deionized water. Baseline offset for clarity. The greatest enhancement in this case was seen with Au NT-SnO<sub>2</sub>-2.

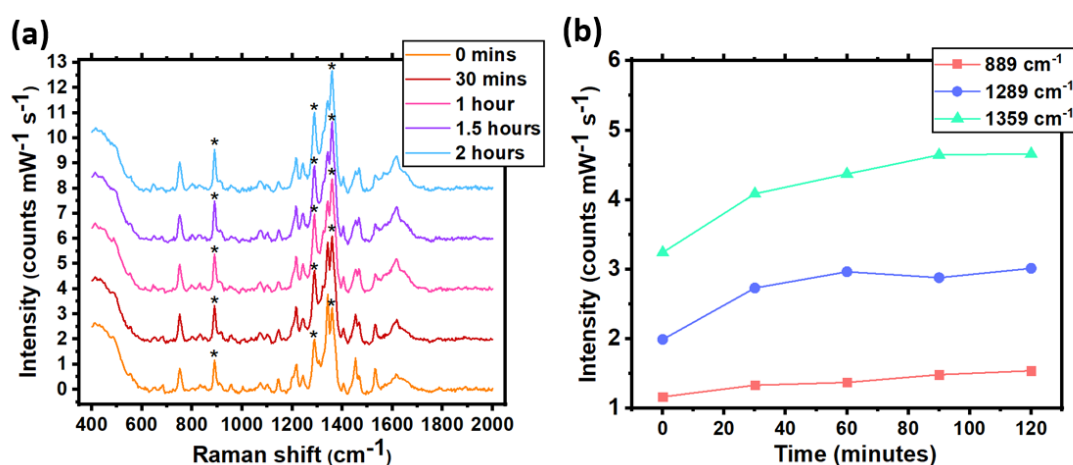


Figure S22: (a) PIERS spectra of 20  $\mu\text{M}$  DNT in Au NT-SnO<sub>2</sub> over 2 hours of UV illumination and (b) Raman intensity vs time plot. Solutions were irradiated in situ over the course of 2 hours with 365-nm UV LED light while PIERS measurements were performed at specific time lapses. Solvent is deionized water.

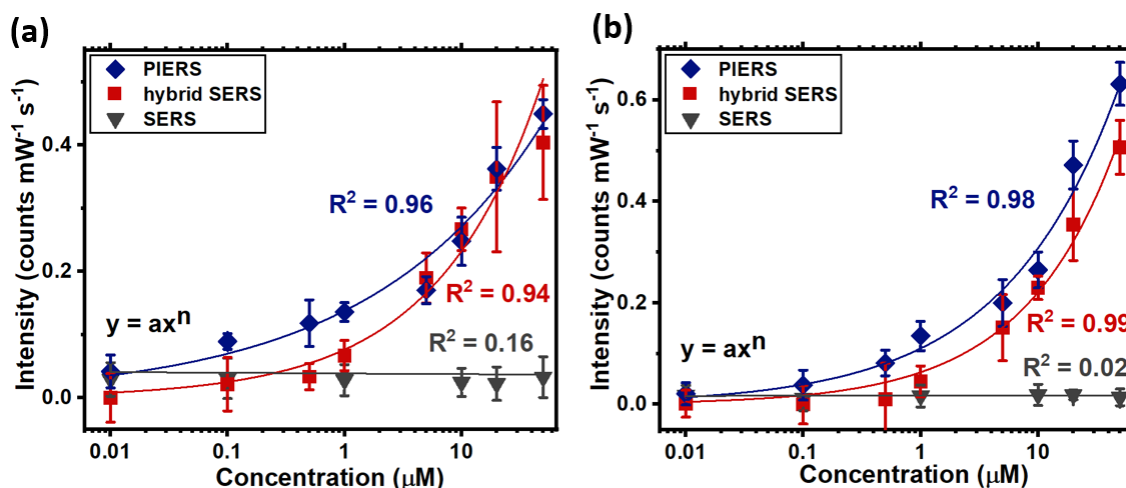


Figure S23: Plot of the SERS, hybrid SERS, and PIERS intensity against DNT concentration (a) for the  $889 \text{ cm}^{-1}$  peak (PIERS  $y = 0.14x^{0.29}$ , hybrid SERS  $y = 0.08x^{0.48}$ ) and (b) the  $1289 \text{ cm}^{-1}$  peak (PIERS  $y = 0.11x^{0.45}$ , hybrid SERS  $y = 0.06x^{0.54}$ ). SERS was measured using Au NTs, and hybrid SERS and PIERS using Au NT-SnO<sub>2</sub>-2. Solutions were irradiated for 2 hours with 365-nm UV light prior to PIERS measurements. Solvent is deionized water, and Au NTs are in 17 mM aqueous CTAC.

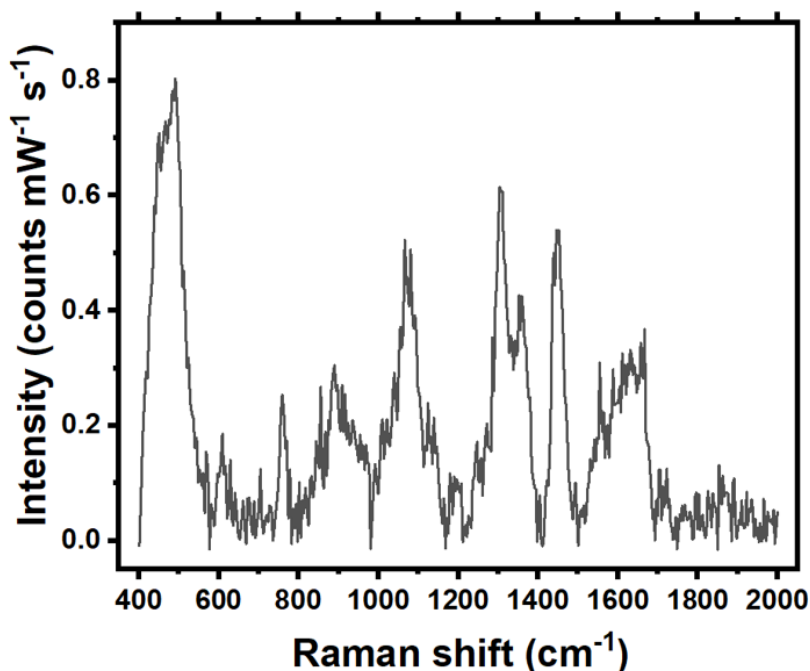


Figure S24: Raman spectrum of CTAC powder.

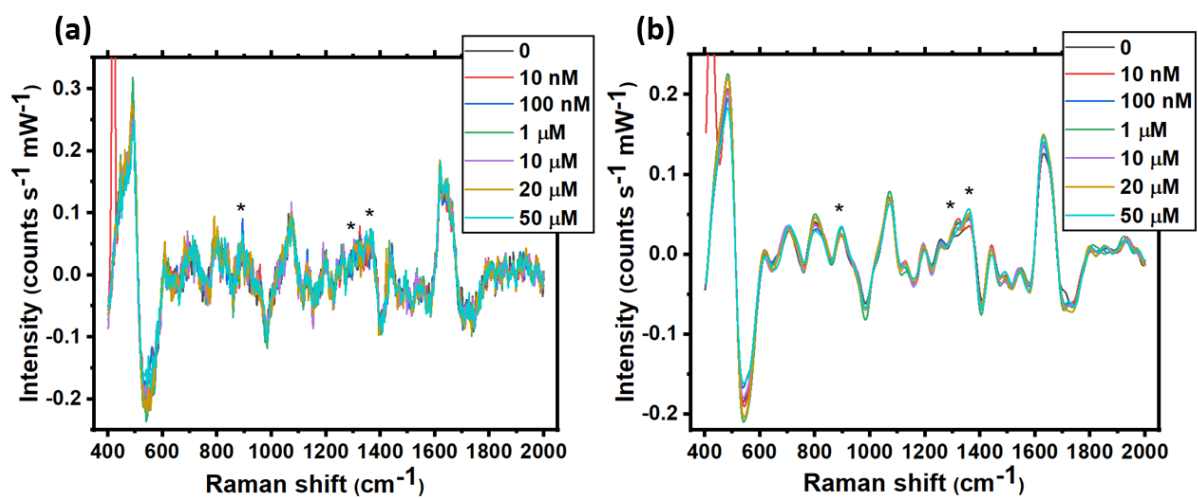


Figure S25: SERS spectra of 2,4-DNT (a) before and (b) after background noise removal using an FFT filter. Solvent is 17 mM aqueous CTAC.

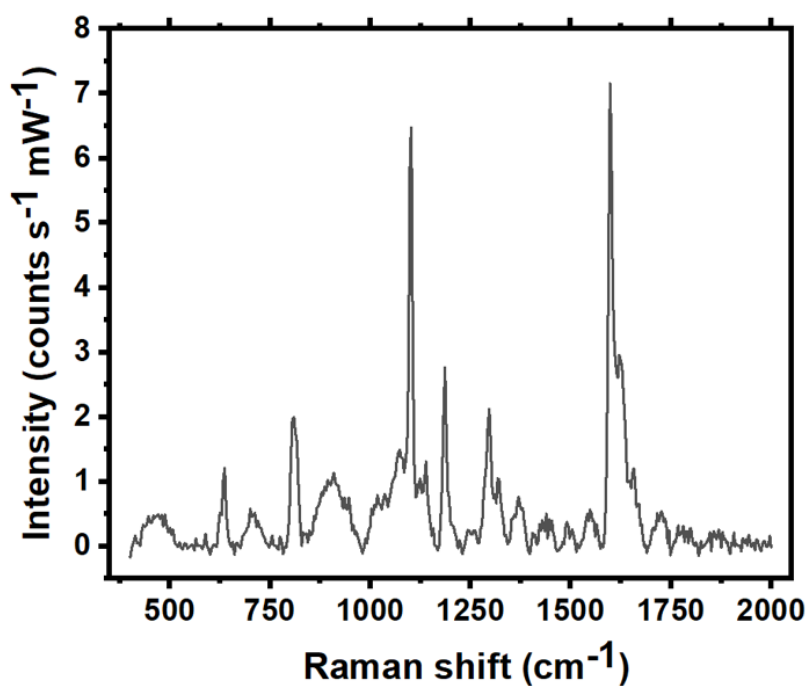


Figure S26: Raman spectrum of 4-MBA powder.

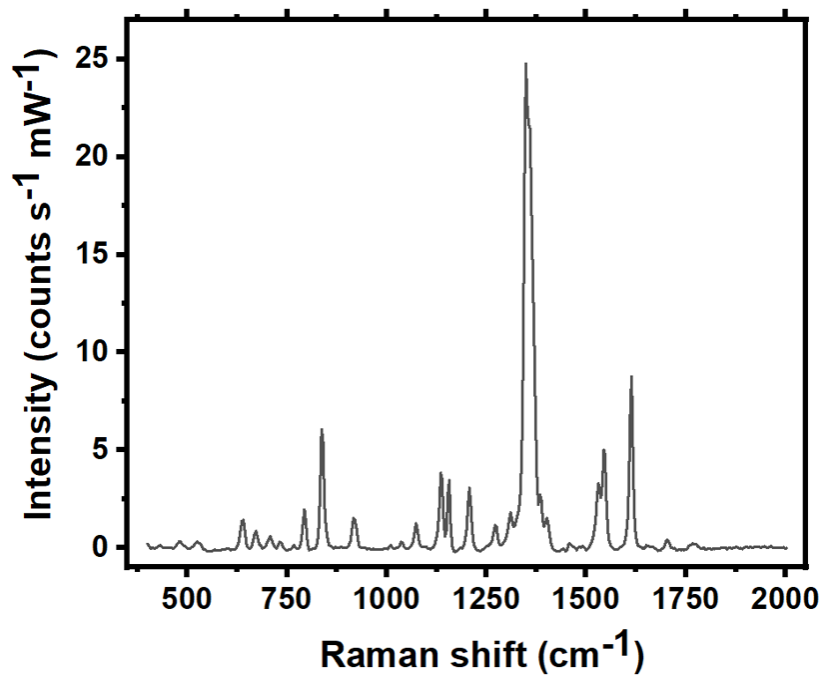


Figure S27: Raman spectrum of 2,4-DNT powder.

## References

- [1] L. Chen, F. Ji, Y. Xu, L. He, Y. Mi, F. Bao, B. Sun, X. Zhang, Q. Zhang, *Nano Lett.* 2014, **14**, 7201.
- [2] G. Oldfield, T. Ung, P. Mulvaney, *Adv. Mater.* 2000, **12**, 1520.